TRANSVERSE JET PENETRATION IN SUPERSONIC FLOWS WITH VARIABLE BOUNDARY LAYER THICKNESS

By

RON PORTZ

A THESIS PRESENTED TO THE GRADUATE SCHOOL
OF THE UNIVERSITY OF FLORIDA IN PARTIAL FULFILLMENT
OF THE REQUIREMENTS FOR THE DEGREE OF
MASTER OF SCIENCE

UNIVERSITY OF FLORIDA

2005

ACKNOWLEDGMENTS

This work was performed with support from NASA grant NCC3-994 with Claudia Meyer as the Program Manager.

Dr. Corin Segal, of the Department of Mechanical and Aerospace Engineering provided direction for this research and contributed valuable guidance in the preparation of this thesis.

Utmost thanks are due my wife Pamela and our children Elijah and Sammy, who have borne with the vicissitudes of life with a graduate student. I am grateful for my parents' confidence and support of me and my family from birth. I would also like to thank my mother-in-law and father-in-law, who in addition to letting me marry their daughter have been of emotional and material support.

TABLE OF CONTENTS

LIST OF TABLES

LIST OF FIGURES

Abstract of Thesis Presented to the Graduate School
of the University of Florida in Partial Fulfillment of the
Requirements for the Degree of Master of Science

TRANSVERSE JET PENETRATION IN SUPERSONIC FLOWS WITH VARIABLE BOUNDARY LAYER THICKNESS

By

Ron Portz

December 2005

Chair: Corin Segal
Major Department: Mechanical and Aerospace Engineering

Penetration of gases injected transversely into a supersonic air stream was measured over varied conditions of fuel molecular weight, relative air boundary layer thickness and Mach number to verify and complement previous studies. Air Mach numbers of 1.6 and 2.5 were tested and compared to published data from Mach 1.5 to 4. Boundary layer thickness was measured and jets of 1 mm, 1.5 mm, and 3.2 mm diam. were injected in a test section with a square section 25 mm wide, followed by a 450 mm long constant area duct. Hydrogen, helium and argon were injected to observe the effects of density and viscosity on penetration. Schlieren imaging was used to visualize and measure penetration. This study compared penetration to existing models using dynamic pressure ratio, air Mach number and boundary layer thickness as independent variables.

Significant penetration dependence on air Mach number was identified. Penetration was found to increase strongly with boundary layer thickness at low Mach numbers but as Mach number increases, boundary layer thickness has less effect. A new

formula is proposed to predict penetration based on a set of independent variables. This formula is compared to new test data and previous results and achieves good correlation for all studies.

CHAPTER 1
INTRODUCTION

When a gas is injected transversely into a supersonic air stream, significant shock and viscous interactions occur. The results of these interactions are not always intuitive as has been shown for external flows,[1,2] and are strongly affected by the ratio of injectant to air dynamic pressures,

$$\frac{q_j}{q_a} = \frac{\rho_j U_j^2}{\rho_a U_a^2}, \tag{1}$$

where jet properties are taken at the jet exit and air properties are for the freestream before encountering jet-induced shocks. The dynamic pressure ratio is used in lieu of the momentum flux ratio in most of the literature on this subject and the terms are sometimes considered interchangeable. The momentum flux ratio is only truly equal to the dynamic pressure ratio if the areas through which the respective fluids pass are equal, which is virtually never the case. Regardless, the dynamic pressure ratio has come to be an accepted datum for the empirical correlation of transverse jet penetration.

In most circumstances the injected plume acts almost as a solid object resulting in the generation of a bow shock, turbulent shear layer and a system of vortices spilling off the semi-cylindrical obstruction, as shown in Figure 1-1. The injectant is turned nearly parallel to the air within a short distance and the vortices' rotation axes align nearly with the air stream. Mixing of the injectant with the air is facilitated by the streamwise vortices spilling off of the turned injectant plume. Near-field mixing is dominated by

bulk mass transfer and the far field mixing by the development of compressible shear layers.

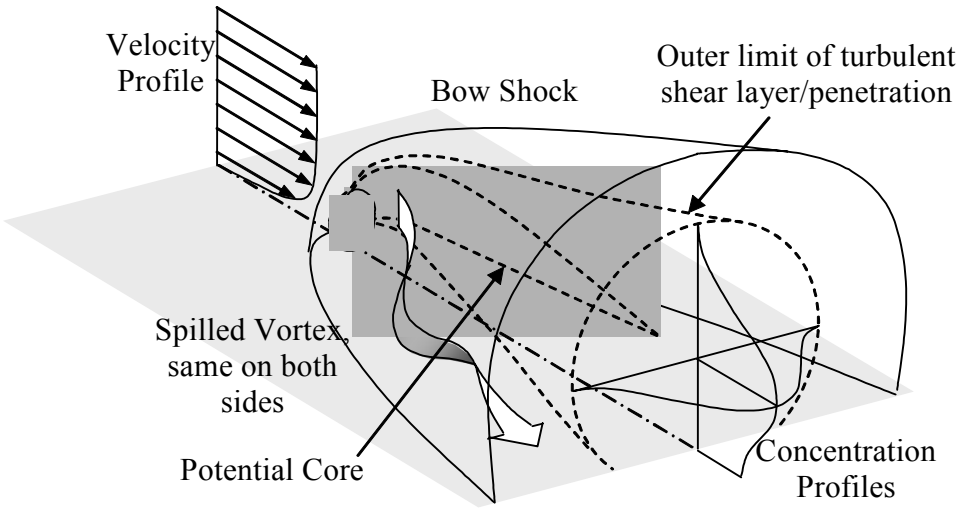

Figure 1-1. Model of Transverse, Underexpanded Injection into a Supersonic Airstream.

Two general cases of interaction between the jet and the boundary layer (BL) have been recognized and are illustrated in Figure 1-2, which is adapted from Schetz and Billig.[3] The determining factor in the shape of the barrel shock around the jet is the degree of BL separation ahead of the jet, which is in turn determined by jet strength compared to freestream properties. When the separation region thickness is much smaller than the height of the Mach disc at the end of the barrel shock, the gas penetrates through the BL and a strong, nearly normal, bow shock forms in the air stream. The barrel shock is bent backward by high pressure air downstream of the bow shock as shown in Figure 1-2A. When the BL separation region is at least of the same order as the first Mach disc height, the jet penetrates straight as shown in Figure 1-2B and as described by Kaufman,[2] Rogers[4] and Schetz and Billig.[3] The Mach disc is nearly parallel to the wall. Kaufman[2] and Schetz and Billig[3] further discuss the criteria that lead to BL separation.

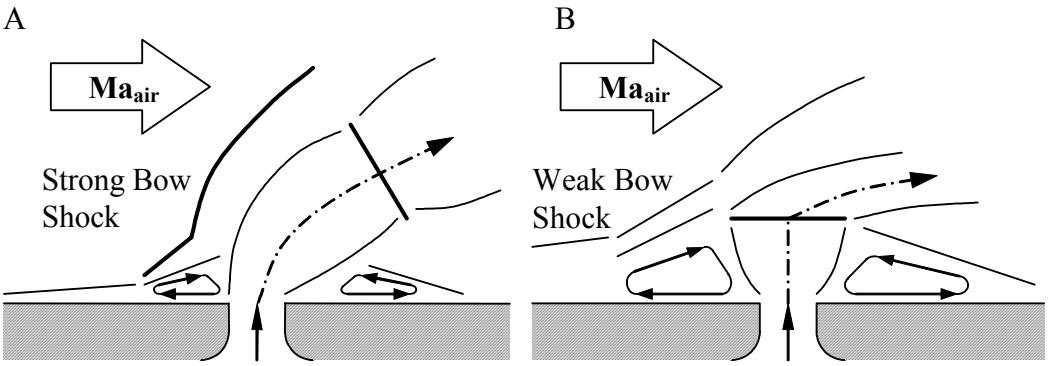

Figure 1-2. Interaction Between the Boundary Layer and Jet in Supersonic Flow. A) Attached and B) Separated Boundary Layer Flows (Adapted from Schetz and Billig[3])

In the case of vehicles with a body-integrated scramjet design, a long inlet ramp with a continuous, strong, adverse pressure gradient is likely to result in a thick BL in the combustor, conducive to flow separation. High stagnation temperature, intrinsic to hypersonic flight, does not facilitate bleeding the BL so this condition becomes of substantial interest.

In a supersonic combustor fuel must penetrate and mix in the cooler high speed core flow beyond the BL to maximize cycle efficiency. Various methods have been suggested such as pylons and ramp injectors to deliver the majority of fuel into the free stream, away from the wall and BL.[5-7] Simple transverse injection is desirable for the sake of simplicity, but it introduces some known disadvantages. The strong shocks that typically accompany transverse injection result in irreversible loss of total pressure in the air. Flameholding is not provided by simple transverse injection and must be provided by combustor features that establish recirculation zones which add to total pressure losses.

Empirically derived models of penetration in supersonic air flows with transverse fuel injection describe the dimensions of the fuel plume penetration and spreading for an injected gas using a definition for the plume boundary based variously on injectant

concentration of 1%, injectant mole fraction of 0.005, intensity of an image, or other criteria, depending on the particular study.[8-10] Different researchers have studied various ranges of experimental conditions and incorporated different sets of independent variables including the dynamic pressure ratio, downstream distance, boundary layer thickness and jet Mach number in the curve fits used to predict penetration. Both jet penetration and boundary layer thickness are usually non-dimensionalized by jet diameter. The variation in definitions and test conditions has resulted in some disagreement in the curve fits produced in previous studies, as will be shown below.

It should be noted that although greater penetration generally results in better mixing, deep penetration is not sufficient to ensure enhanced combustion. For transverse injection tests relying on auto-ignition due to temperature increase across the bow shock it has been observed that cooler air passing through oblique shocks curving off of the bow shock inhibit combustion in zones where the equivalence ratio is otherwise within flammability limits.[11] Results reported in reference 11 indicate that burning was restricted to a small recirculation kernel in the stagnation zone upstream of the fuel jet and in a thin sheet immediately aft of the bow shock where temperatures were high. The majority of the fuel did not react with the air despite good fuel penetration and mixing. Good fuel and air mixing is only one of the factors resulting in efficient combustion.

CHAPTER 2
NEAR FIELD AND FAR FIELD MIXING OF TRANSVERSE JETS

For combustion to occur fuel and air must mix and diffuse at a molecular level. The transport of one molecular species into another is described by Fick's Law[12]

$$\dot{m}_A = Y_A(\dot{m}_A + \dot{m}_B) - \rho D_{AB}\frac{dY_A}{dx} \tag{2}$$

where

- $\dot{m}_A$ is the bulk mass flow rate of species A into species B
- $\dot{m}_B$ is the bulk mass flow rate of species B into species A
- Y_A is the mass fraction of species A
- ρ is the density of species A
- D_{AB}, is the binary diffusion coefficient for species A diffusing into species B defined as

$$D_{AB} = \frac{2}{3}\left(\frac{R_B^3 T}{\pi^3 \mathscr{M}_A}\right)^{1/2}\frac{T}{\sigma^2 P} \tag{3}$$

where

- R_B is the gas constant for species B, T is the temperature,
- $\mathscr{M}_A$ is the molecular mass of species A,
- σ is the molecular collision diameter, or weighted average of the diameters of molecules A and B
- P is the pressure.

The first term in (2), $Y_A(\dot{m}_A + \dot{m}_B)$, is the bulk flow of species A into B and does not result directly in molecular mixing. The second term, $-\rho D_{AB}\, dY_A/dx$, shows that the diffusive mass flow rate of species A into B increases with increasing density, binary diffusion coefficient and species gradient. Inspection of (3) reveals that the diffusion coefficient increases with temperature to the $\frac{3}{2}$ power, with pressure to the -1 power, molecular weight of species A to the -$\frac{1}{2}$ power and molecular diameter to the -2 power. For perfect gases the overall mass flow rate due to diffusion changes with the square root of temperature, and is neutral for pressure changes. The overall rate of diffusion is maximized for small, light molecules at high temperature. Intuitively, this is due to increasing average molecular speed while decreasing the rate of collision between the diffusing gas molecules. Frequent collisions impede the average motion of molecules in the direction of decreasing concentration. This contributes to the preference of hydrogen to fuel supersonic combustion; in addition to the rapidity of reaction associated with hydrogen once it has mixed with oxidizer, it will diffuse and mix more quickly in air than any other fuel due to its small molecule size.

Once a design flight condition is chosen which fixes engine inlet temperature and pressure and a fuel is selected there are limited options for the combustor designer to affect diffusion. For this reason it turns out that controlling bulk flow processes dominates the eventual mixing efficiency of fuel injected into a supersonic air stream. When a gas is injected transversely into an air stream non-linear penetration is apparent in the near field. Large momentum flux transfer between the air and the jet dominates the penetration and mixing process. Bulk mass transfer is brought about by significant jet penetration. In some studies[4, 9] greater lateral spreading than axial penetration was

noticed for transverse fuel injection indicating that the shear forces due to the vortices spilling off of the side of the fuel jet were a more effective transport mechanism than the transverse injection momentum.

In the far field, more than ten jet diameters downstream of the injection location, penetration increases by essentially tangential shear layer growth where the penetration distance assumes a nearly linear relationship with downstream distance. In this regime the jet centerline is essentially parallel to the air and the slope of the penetration curve is directly related to the shear layer growth.[13] For practical supersonic combustors and the test equipment employed in this study the Reynolds number exceeds 10^6. At Reynolds numbers above 10^4 the shear layer is turbulent with macroscopic vortex structures moving at a convective velocity, U_c, defined as.[13]

$$U_C \equiv \frac{U_2 a_1 + U_1 a_2}{a_1 + a_2} \tag{4}$$

where U_i and a_i are respectively the velocity and speed of sound of each of the fluids. The convective Mach numbers, M_{ci} for two fluids are defined as

$$M_{C1} \equiv \frac{U_1 - U_C}{a_1} \text{ and } M_{C2} \equiv \frac{U_C - U_2}{a_2} \tag{5}$$

Shear layer growth is a function of the ratio of fluid velocities, the ratio of fluid densities and M_c.[13] The shear layer growth rate decreases with increased compressibility and increases with increased density ratio between the two fluids. For a detailed discussion of mixing in shear layers, see reference 13.

Enhanced mixing schemes have been described elsewhere[14, 15] which convert some of the tangential momentum of the air into transverse momentum along with generation of vortical structures. An example is the swept ramp injector in which air passes over an

upward incline adjacent to either a flat or a downward inclined surface.[16-18] Spillage from the ramp creates a vortex that enhances bulk fuel flow into air while causing oblique shocks and relatively small losses unlike simple transverse injection which produces normal shocks and strong vortices that result in significant stagnation pressure loss. Angled injection from a wall has been studied with the intent to retain the simplicity of transverse injection while minimizing the stagnation pressure loss.[7, 18]

Studies with gaseous hydrogen as the injected fuel have observed that significant additional thrust results from injection of fuel with a tangential velocity component.[18] Tangentially injected fuel will contribute some small thrust and the specific impulse of hydrogen may be high if it is used to cool hot engine parts before injection. However, the thrust addition is minor, because of the small fuel mass involved, for example ~3% H_2 by mass at stoichiometric mixture ratio.

Both near and far-field mixing mechanisms are present in both transverse and angled jet injection. Deep penetration facilitates mixing and with appropriate flame-holding devices promotes efficient supersonic combustion chambers. The results of experimental penetration analysis and its correlation to the jet flow thermodynamic properties of gaseous jets are described below.

CHAPTER 3
EXPERIMENTS

Experimental Facility

Figure 3-1 is a schematic representation of the continuous-flow, direct-connect, supersonic-combustion wind tunnel used in these experiments. This tunnel can deliver .454 kg/s of air continuously at combustor Mach numbers from 1.3 to 3.6, with stagnation temperature up to 1,200K and stagnation pressure from 207 to 827 kPa. Higher flow rates and pressures up to 1,520 kPa are subject to limited duration. These conditions correspond to flight enthalpy of up to Mach 4.75. This facility has been previously described in detail by Owens.[5]

For the purpose of measuring jet penetration this study used unheated air, consistent with previous studies.[4, 9, 10, 18] The entrance to the test section was an L = 25.4 mm wide square section. The cross-section was constant along its length of 18L. Hydrogen, helium or argon were injected transversely, at a location where the BL thickness was known, through 1 mm, 1.5 mm, and 3.2 mm orifices to vary the ratio of BL thickness, δ, to jet diameter, D.

Boundary Layer Thickness

BL thickness was measured using a probe with a square-cut tip of 0.25 mm outside diameter, and 0.13 mm bore diameter. The probe was inserted through any of three holes in the side-wall of the test section normally used for optical access (see Figure 3-1) and was traversed in 0.2mm increments while measuring the stagnation pressure. Measurements were taken around the isolator outlet circumference for unheated air at 414

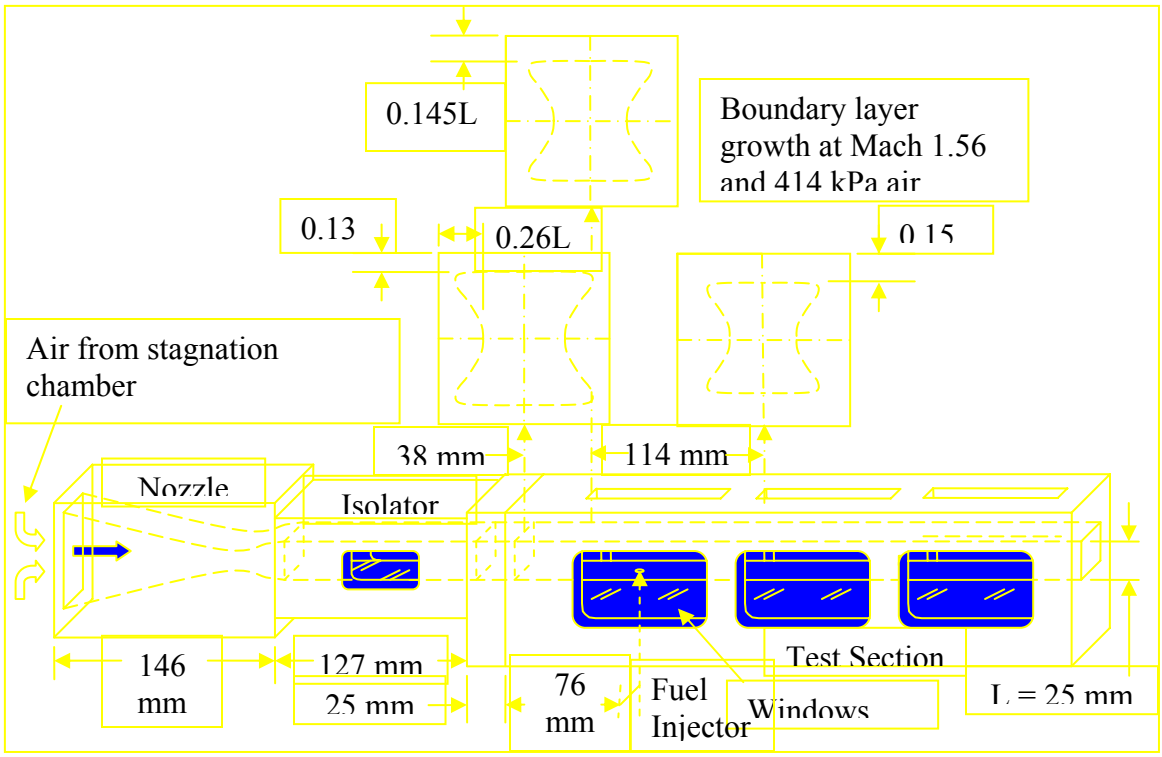

Figure 3-1. Schematic of the test section with dimensions normalized by duct height, L=25 mm. The measured BL at selected locations is also shown.

kPa stagnation pressure and nozzle exit Mach number of 1.6. The results of this measurement are shown in Figure 3-2. Lack of physical access to the East side of the test apparatus restricted BL measurements to three sides. Symmetery of the apparatus ensures that use of the West-to-East BL measurement accurately represents the East-to-West BL. The BL measurement was repeated in the West-to-East direction at both Mach 1.6 and Mach 2.5. Fuel is injected from the East wall. The BL was measured at several stations downstream of the nozzle exit, as indicated in Figure 3-2. Measurements showed a relatively small inviscid core flow at the point of injection since the measured BL occupies over 50% of the cross section area. At Mach 1.6 BL growth in the 18L long constant-area test section resulted in choking unless a substantial bleed from the last third of the test section was established. At each station, the BL thickness is taken as the point

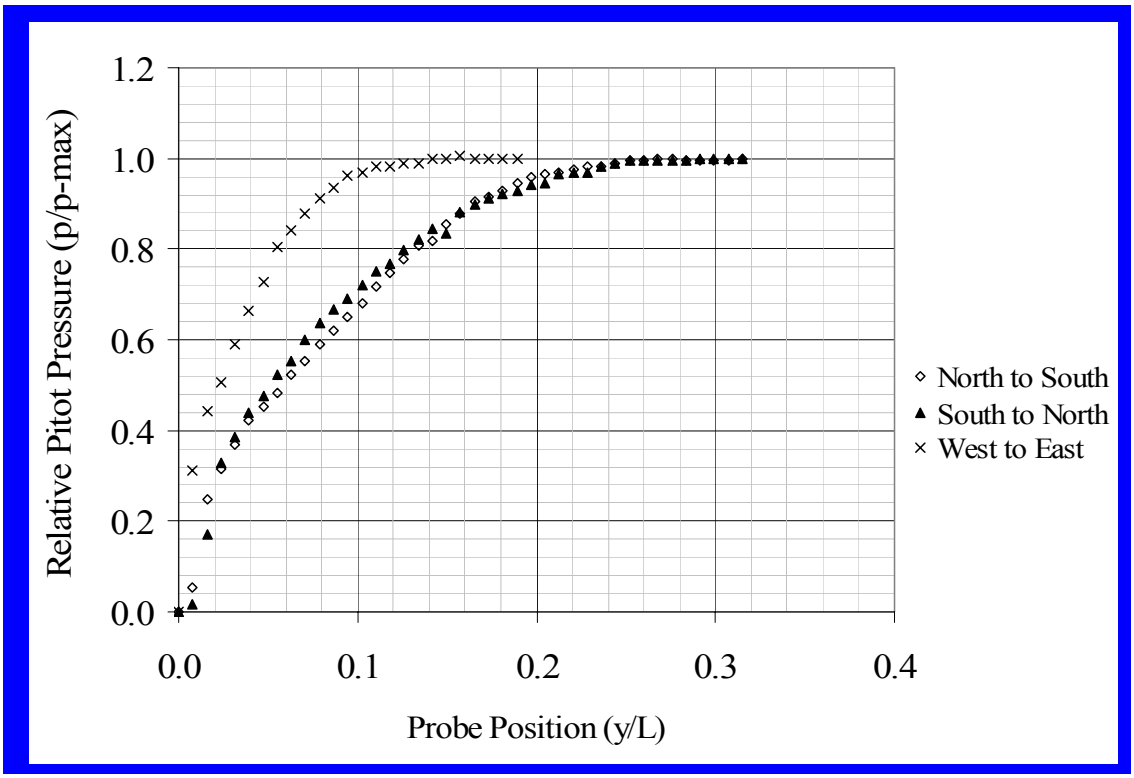

Figure 3-2. Boundary layer measurement at the collar outlet. The collar exit is 76 mm, or 3L upstream of the fuel injector. Measurements are taken from the outside edge toward the center of the flow, along the section centerline. The cardinal directions are used as references.

of 99% velocity, or where the measured pitot pressure was 98% of the maximum value. The BL thickness at the point of gas injection was approximated by linear interpolation between the two stations measured on either side of the port as shown in Figure 3-3. For 552 kPa stagnation pressure and Mach 1.6 flow, the BL thickness at the injector port was 3.7 mm. For Mach 2.5 flow the BL thickness was 2.5 mm.

It is known from measurements taken here and elsewhere[19] that rectangular, 2-D nozzles yield boundary layers that are not uniform around the passage circumference. Along the contoured nozzle walls, the boundary layer is uniform in thickness and thinner than on the flat walls of the 2-D nozzle. The flat walls have a non-uniform BL as shown in Figure 3-1, with greater thickness at the center than at the edges, where BL thickness is

similar to the contoured walls. At the station 1.75L forward of the point of gas injection, the BL thickness was 3.3 mm on the contoured walls, while the maximum BL thickness on the flat walls was 6.6 mm. This is due to the stronger favorable pressure gradient along the contoured walls.

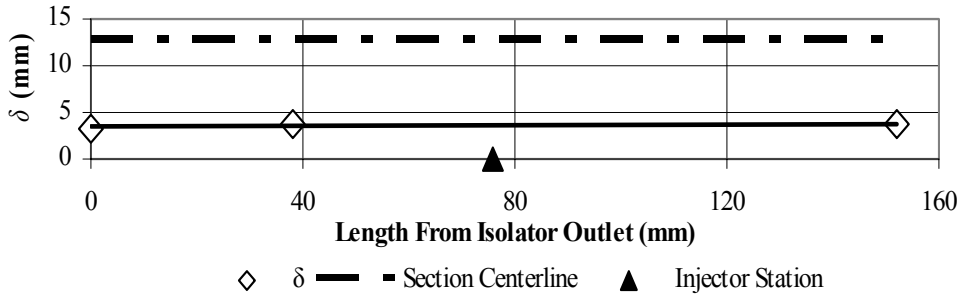

Figure 3-3. The BL at measured locations bounding the injector port and assuming linear growth.

CHAPTER 4
RESULTS AND ANALYSIS

Penetration Visualization

Flow and fluid mixing are visualized by use of a lens-based Schlieren system. Optical assessment of jet penetration has been demonstrated to give accurate and consistent depth compared to chemical sampling methods.[13, 20] Images were collected with an SVHS video camera. To capture average penetration rather than instantaneous variations each camera exposure was of the order of 20 ms which is long compared to transient flow excursions.

Schlieren systems make flow phenomena and optical irregularities visible by passing collimated light through transparent media. Changes in the refractive index between fluids or between regions where the thermodynamic properties of a fluid change, such as a shock wave, result in light refracting out of collimation. The collimated light is focused onto a sharp edge, which cuts off the refracted light and creates a shadow which shows where the change in species or properties occurs. For an in-depth and wide-ranging discussion of schlieren techniques, see reference 21.

Measuring penetration by visual examination is influenced by the indices of refraction of the air and fuel. The boundary between fluids becomes more distinct as the indices of refraction are more different. The helium/air interface for example is unambiguous with air's index of refraction being 1.000293 and helium's being 1.000036 at 586.3 nm. Argon visualization requires greater sensitivity since its index of refraction, at 1.000281, is very close to air's. Adjustment of the amount of schlieren cutoff to

increase sensitivity was successful in establishing the gas jet boundary with certainty in a minority of cases where argon was injected. Hydrogen's index of refraction is 1.000140, which gives results intermediate between argon and helium. Figure 4-1A shows that

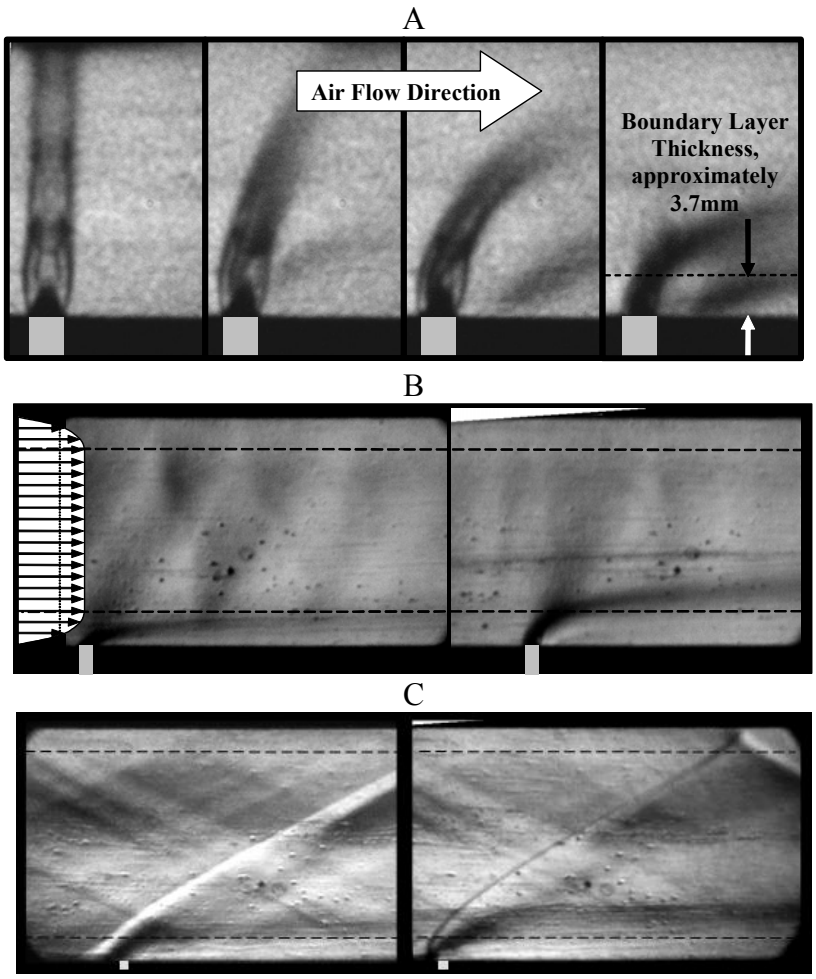

Figure 4-1. Schlieren Images of Underexpanded, Circular, Sonic Gas Injection. A) 3.2 mm He jet at P_0 = 621 kPa. Air velocity increases from 0 to Mach 1.56 at P_{0a}=414 kPa, δ/D=1.16. B) 1.5 mm H_2 jet, q_j/q_a=0.50 (left) and q_j/q_a=1.5 (right) at Ma_a=1.56, P_{0a}=552 kPa, δ/D=2.42. Approximate BL and air velocity profiles superimposed. C) 1 mm H_2 jet, q_j/q_a=1.0 (left) and q_j/q_a=2.5 (right) at Ma_a=2.48, P_{0a}=552 kPa, δ/D=2.54.

determining the injection centerline from the recorded image requires use of the leeward jet exit point as a datum, because the windward exit point is deformed by air stagnation pressure.

The schlieren images in Figure 4-1A make visible the vortex that spills off of the injectant. Figure 4-1A shows helium injected into quiescent air through a 3.2 mm orifice. As air flow increases, a shadow is increasingly visible downstream of and below the jet. This shadow extends far downstream parallel to the flow marking the lower extent of the mixing vortices. When near-field penetration is weaker, as shown in Figure 4-1B, where the jet diameter is 1.5 mm, the jet is turned close to the wall and exits the BL at a shallow angle. The great majority of mixing must occur within the BL. Rogers[4] shows that gas concentrations and spreading are greatest in the BL especially in the near field when the BL is thick. Deeper near-field penetration results in better defined mixing vortices, which are known to enhance spreading and mixing.[22]

Argon, hydrogen and helium gas were transversely injected into the supersonic flow through circular orifices of 1.0 mm, 1.5 mm, and 3.2 mm diameter. Inspection of the schlieren images shows that the windward side of the gas plume is deflected at an angle downstream from the normal direction by subsonic air close to the wall, but that the lee side of the jet is not deflected. The supersonic free stream is presented with an oblique obstacle, resulting in a weaker oblique shock wave displaced from the wall, as shown in Figure 4-1B.

Gases injected into a Mach 1.6 air stream do not penetrate far beyond the boundary layer if the jet diameter is less than half the BL thickness and q_j/q_a is no more than 1.5, as shown in Figure 4-1B. For Mach 1.6 air, the classic picture of the bow shock is not accurate when the BL is significantly thicker than the injector diameter. At the point in the BL where oncoming air is supersonic the injected plume has already turned, presenting the air with an oblique obstacle that does not span the test section, resulting in

a weak shock structure that is only minimally visible. The outer edge of the plume is identified on the Schlieren image by a band where light has been refracted away leaving an outline of the plume edge as shown in figures 4-1A, B and C.

For Mach 2.5 flow, shown in Figure 4-1C, a distinct bow shock is visible and the interaction of the bow shock with the boundary layer is visible. This is consistent with higher Mach number in the BL and the reduced measured BL thickness.

The depth of argon, helium and hydrogen penetration is presented in Figure 4-2 as a function of a correlation of independent variables considered to have an effect on gas penetration for measurements taken at Mach 1.6. The relative importance of each variable is modified by exponents that were determined empirically to minimize the summation of the squared relative data scatter about the mean power-law curve. Penetration was expressed as P/D, the depth of penetration divided by the jet exit diameter. The independent variables most commonly represented in literature are the dynamic pressure ratio between the jet at its exit and the air freestream and the downstream distance ratio at which penetration was measured, *x/D*. Additional variables that may affect penetration are the BL thickness ratio, *δ/D*, the ratio of jet to air Reynolds numbers and the ratio of jet to air molecular weight.

The resulting penetration formula, based on the data gathered in the present study, is

$$P/D = 1.362(q_j/q_a)^{0.568}(x/D - 1.5)^{.276}(\delta/D)^{.221}(\mathrm{Re}_j/\mathrm{Re}_a)^{-0.0084}(\mathcal{M}_j/\mathcal{M}_a)^{-0.025} \quad (6)$$

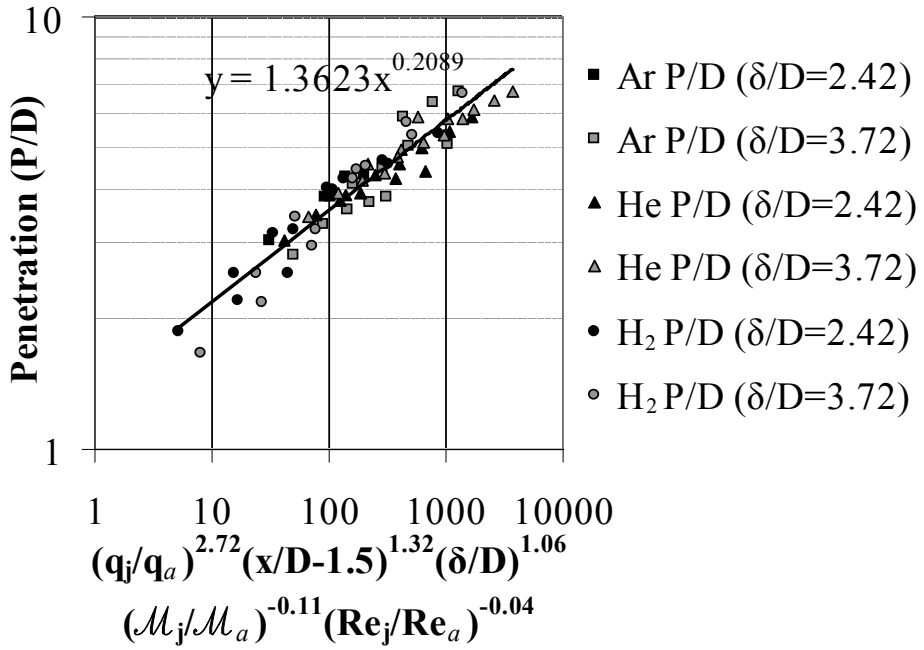

Figure 4-2. Curve Fit for Ar, He and H_2 injection into Mach 1.6 air at Varied BL thickness.

Effect of Dynamic Pressure Ratio and Downstream Distance

The ratio of jet to air dynamic pressure has the strongest effect on penetration of the variables examined. Figure 4-3 shows how varying q_j/q_a from 1 to 4 over x/D from 0 to 30 with the other variables held constant results in significant changes to the curve predicted by eqn. 6. Here M_a=2.0, δ/D=2 and $\mathcal{M}_j/\mathcal{M}_a$=0.070. The effect of x/D is also apparent in Figure 4-3. Near-field penetration increases quickly with increasing x/D, but far-field penetration increases relatively slowly and beyond ~10D almost linearly with increasing x/D.

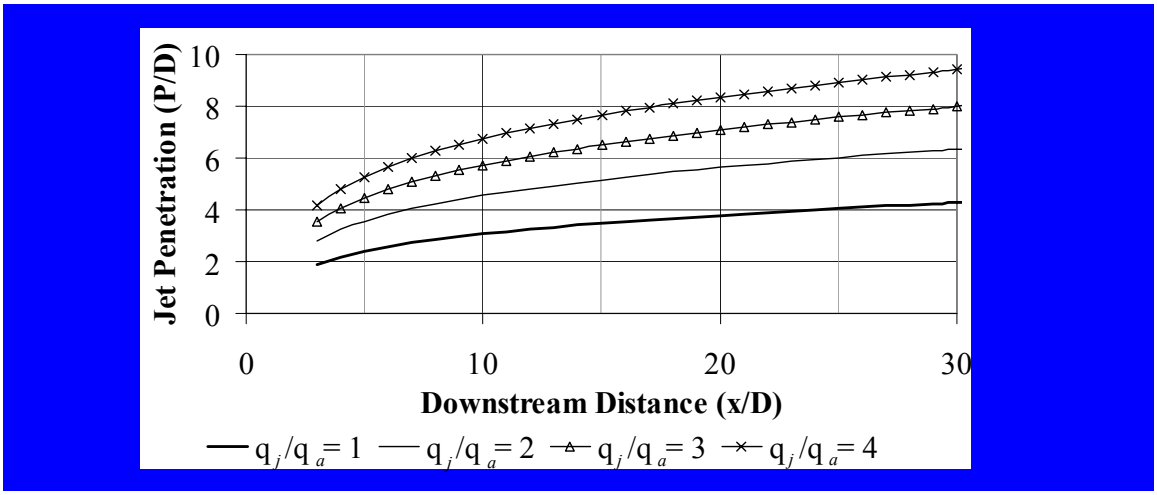

Figure 4-3. Penetration Varies Greatly With Increasing Dynamic Pressure Ratio. M_a=2, δ/D=2, $\mathcal{M}_j/\mathcal{M}_a$=0.070.

Effect of BL Thickness

The thickness of the BL will effect jet penetration as shown in Figure 4-4. Increasing δ/D results in increased penetration into Mach 1.6 air. The degree by which penetration is increased decreases with increased air Mach number. When the supersonic Mach number is high much of the BL flow is also supersonic. The bow shock within the BL is strong with downstream conditions similar to conditions downstream of the free stream bow shock.

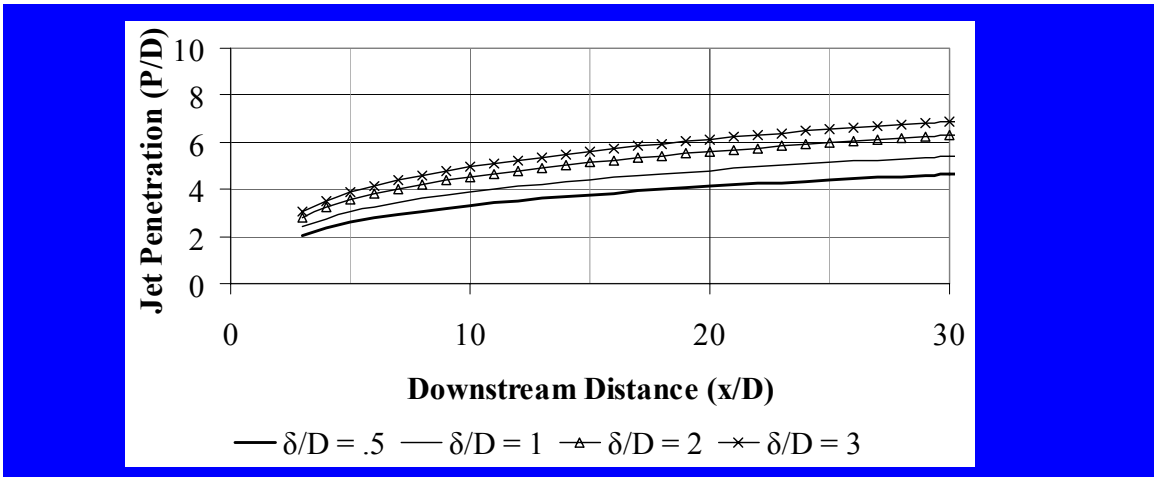

Figure 4-4. Penetration Variation with BL Thickness. M_a=1.6, q_j/q_a=2, $\mathcal{M}_j/\mathcal{M}_a$=0.070.

Effect of Molecular Weight Ratio

The effect of variation in molecular weight is illustrated in Figure 4-5. This figure shows that variation of injecant molecular weight has very little effect on penetration. As a result the exponent applied to the molecular weight is small and hydrogen penetrates nearly as far as argon which has a molecular mass 20 times greater. This is similar to the result of Torrence's study.[23] Torrence found that at x/D=30 argon penetrated slightly deeper than hydrogen or helium, in agreement with the present study, but also found a minimium at intermediate molecular weights, which the resolution of the present study did not reveal. Torrence also found that the most significant affect of molecular mass was to decrease lateral spreading with increasing molecular mass while the depth of maximum penetrant concentration was essentially unaffected.

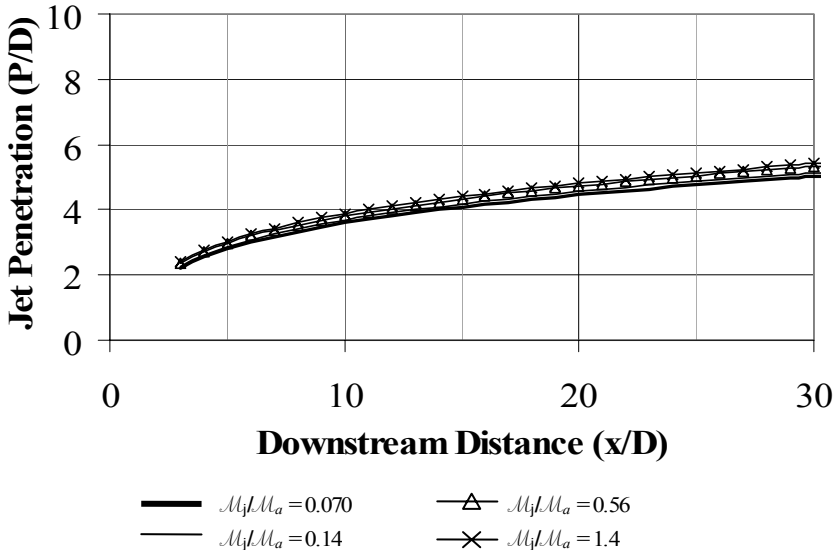

Figure 4-5. Variation in Penetration Due to Variation in Injectant Molecular Weight. M_a=1.6, q_j/q_a=2, δ/D=1.

The Reynolds number ratio has an exponent very close to zero indicating negligible effect. It was therefore considered reasonable to drop any Re dependence and eqn. 6 becomes,

$$P/D = 1.362(q_j/q_a)^{0.568}(x/D - 1.5)^{.276}(\delta/D)^{.221}(\mathcal{M}_j/\mathcal{M}_a)^{-0.025} \qquad (7)$$

Povinelli and Povinelli[24] included a function of the ratio of air to jet Mach number in the correlation function which was not considered in the present study since only sonic injection was considered here. In their study as well as in a study by Billig, et al.,[25] the effect of supersonic fuel injection was considered weak.

CHAPTER 5
A PROPOSED, IMPROVED PENETRATION FORMULA

Comparison To Previous Studies

Figure 5-1 shows plots resulting from empirical formulae for predicting the outer limit of jet penetration that resulted from this and several previous studies of transverse injection. Each of these tests was conducted at different conditions which has affected the results. Schetz and Billig[3] analytically predicted transverse penetration at the centerline of an injected flow using the momentum transfer for a non-deforming plug. Their results are also plotted in Figure 5-1. In the analytical model of Schetz and Billig the injected plug of fluid carries transverse momentum into the air stream which initially has zero transverse momentum. This fluid particle is accelerated by transfer of momentum from the air stream to the particle while the air stream reacts by receiving and dissipating transverse momentum from the jet and converting some of its linear momentum to transverse momentum primarily in the form of the spilled vortices.

Equation (7) determined in this study agrees well with the results of Leuchter[8] and Hersch, et al.[20] at q_j/q_a=1.5 however there are differences between these results and the other studies. The curve of Schetz and Billig[3] identifies the injected jet centerline whereas all others identify the outer limit of gas penetration. This curve is complemented with another curve marking ½ jet diameter from the analytical centerline, which is maintained constant at all x/D for simplicity as in the study by Billig et al.[25] The curve of Schetz and Billig[3] plus ½ jet diameter approaches the present study in the far field, beyond x/D=20.

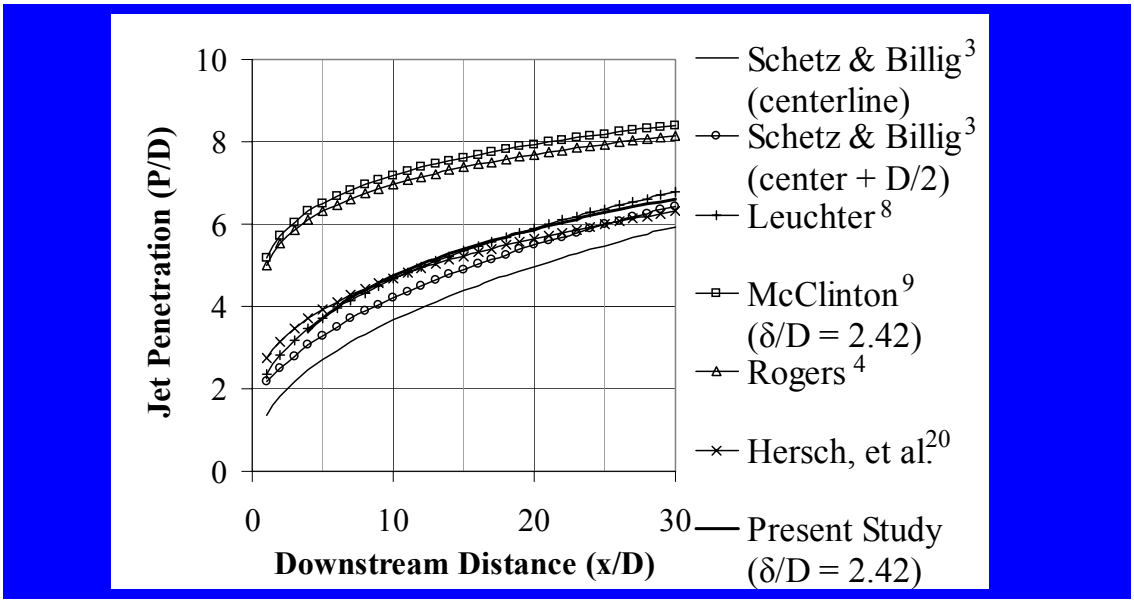

Figure 5-1. Penetration Correlations for Various Studies Exhibit Scatter; q_j/q_a=1.5.

One factor that will influence the penetration measurement is the definition of the outer limit of penetration, which varies between studies. Near the penetration limit the concentration gradient is shallow as shown by Rogers[4] so any variation in definition can affect the measured penetration. This effect is assumed to be small for comparing the results of different studies and for generating an engineering estimate of penetration.

The test conditions employed by each researcher affect the derived correlation. For example the correlation of Leuchter[8] is very similar to the formula derived in this study. Leuchter's test condition of Mach 1.5 corresponds closely with the Mach 1.6 flows that dominate the data gathered for this study. Studies performed at Mach 2 freestream conditions resulted in slightly deeper prediction of penetration and studies at higher air Mach numbers indicated further penetration increases. This dependence is stronger than the ratio of jet to freestream Mach number effect found by Povinelli and Povinelli[24] and by Billig, et al.[25] because their work varied the injector rather than the freestream Mach number to specifically investigate that particular effect while leaving any shock

interactions in the air stream essentially unaffected. It may be concluded that there is a relationship of penetration with air Mach number that has previously not been accounted for.

General Penetration Formula

A generic form for the penetration equation used in any of the studies cited above is

$$P/D = A\left(q_j/q_a\right)^B (x/D + C)^E (\delta/D)^F \left(\mathcal{M}_j/\mathcal{M}_a\right)^G \tag{8}$$

Table 5-1. Penetration Formula Parameters Resulting From Various Studies

	A	B	C	E	F	G	Mach No.
Schetz and Billig[3]	1	0.435	0	0.435	0	0	N/A
Leuchter[8]	1.45	0.5	0.5	0.35	0	0	1.5
Hersch. et al.[20]	1.92	0.35	0.5	0.277	0	0	2
Rogers[4]	3.87	0.3	0	0.143	0	0	4
McClinton[9]	4.2	0.3	0	0.143	0.057	0	4
Present study	1.36	0.568	-1.5	0.276	0.221	-0.0251	1.56

The values for each of the terms, A, B, C, E, F and G were placed in Table 5-1, along with the air Mach number of the tests used to derive the formula. Since a trend in experimental data was noticed as the air Mach number changed, the values of the exponents in equation (8) were plotted versus air Mach number and curves were fit to these values as shown in Figure 5-2. Linear curves were used in all cases except for term "E" which was better fit with a power law curve due to a rapid change at lower Mach numbers and more gradual change at higher Mach numbers. A refinement of the

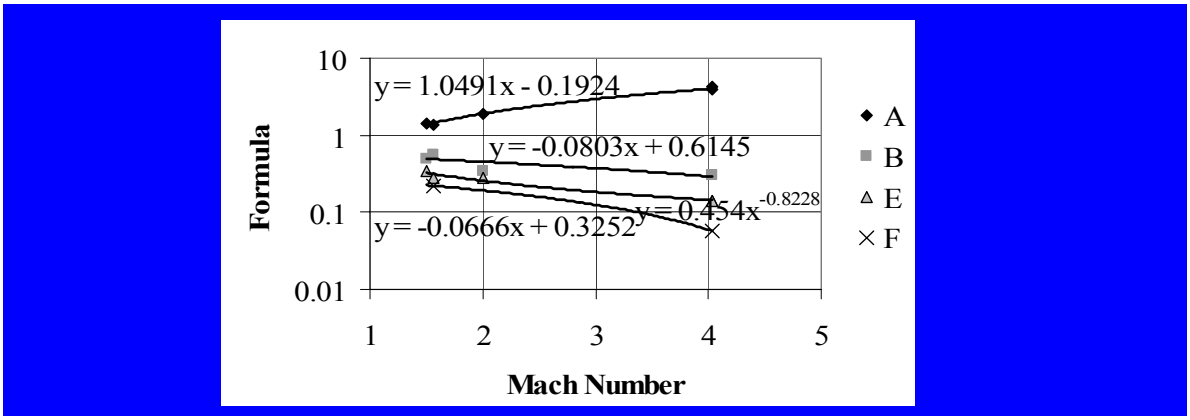

Figure 5-2. Penetration Equation Parameters versus Air Mach number.

constants derived from Figure 5-2 was needed when fitting test data to the formula most likely due to the relatively small sample size used to derive the correlations in Figure 5-2. Insufficient data were available to establish a Mach number relation for G so the constant derived in the present study is used as shown in Table 5-1. The functional forms of A, B, C, E and F are shown in Table 5-2.

Table 5-2. Penetration Equation Parameters as Functions of Air Mach number.

Coefficients for Equation (8)	Function of Air Mach Number, M_a
A =	1.0491 M_a – 0.1924
B =	-0.0803 M_a + 0.6145
C =	-2.34/M_a
E =	0.395 M_a -0.8228
F =	-0.0666 M_a + 0.3252
G =	-0.02507

The resulting equation is

$$P/D = (1.05M_a - .192)(q_j/q_a)^{(-.0803M_a+.615)}(x/D - 2.34/M_a)^{.395M_a-.823}(\delta/D)^{-.0666M_a+.325}(\mathcal{M}_j/\mathcal{M}_a)^{-.0251} \quad (9)$$

Figure 5-3 shows good correlation of this formula with all the test results compiled by the other researchers cited here. The inputs to the formula, including Mach number, BL thickness and dynamic pressure ratio are taken directly from test data compiled in the

previous studies and are shown in Figure 5-3. Independent verification with test data obtained in the present study at M_a = 2.5, which was not used to create the formula, is presented in Figure 5-4. Generally good agreement is evident in particular in the midfield. Close to the injection location where the slopes are large or in the far field beyond 30 jet diameters the differences between prediction and test data are much less than one jet diameter.

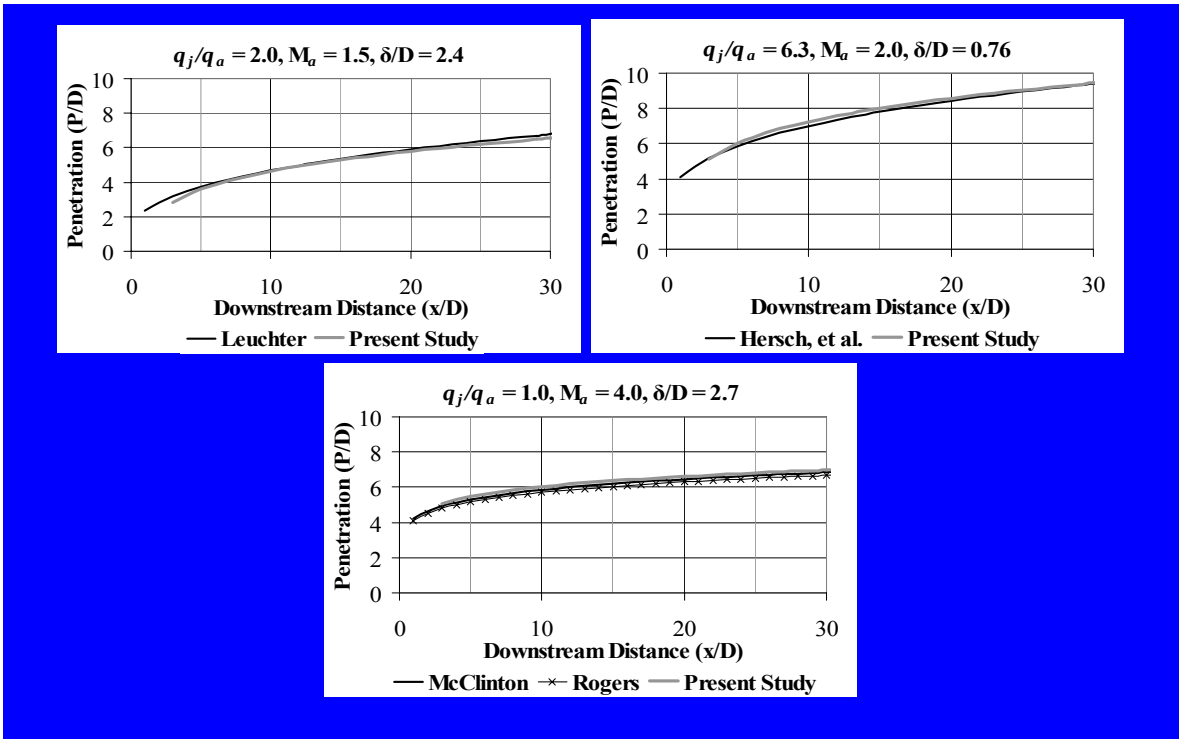

Figure 5-3. Comparison of the Present Study with Previous Research. A) vs Leuchter[8] for H_2; M_a=1.5. B) vs Hersch[20], et al. for He; M_a=2 C)vs Rogers[4] and McClinton[9] for H_2; M_a=4

Examination of equation (9) shows that penetration increases with increased dynamic pressure ratio, downstream distance and BL thickness to jet diameter ratio as expected; the penetration also increases with increased air Mach number which is not intuitively expected.

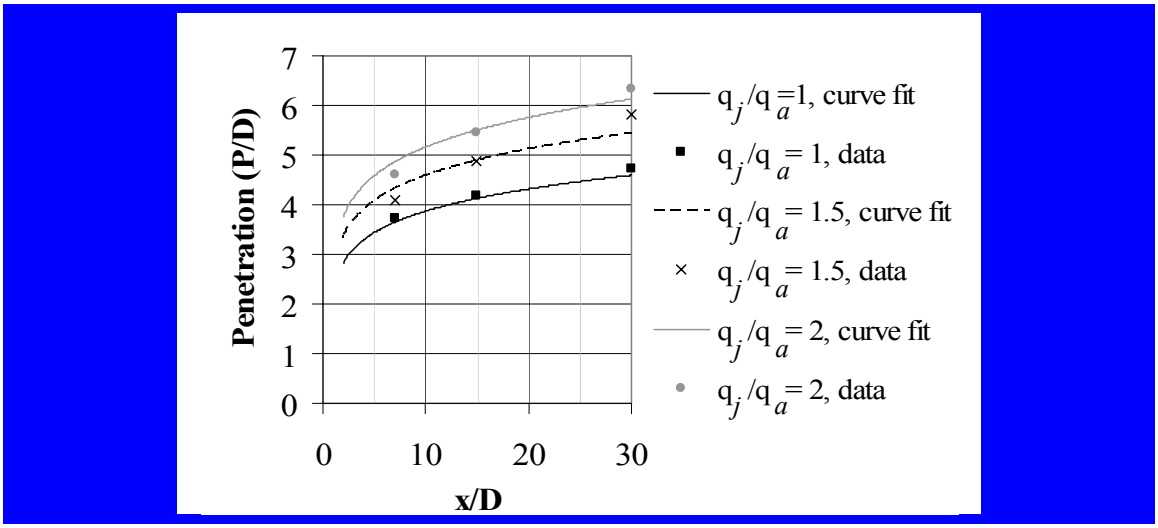

Figure 5-4. Predicted and Measured Penetration of Sonic Hydrogen Transversely Injected into Mach 2.5 Air

The increased penetration due to increased Mach number can be attributed to the stronger bow shock structure associated with higher Mach flows. As shown in Figure 5-6 the dynamic pressure on the downstream side of the shock is an increasingly small percentage of the upstream dynamic pressure as Mach number increases, so the dynamic pressure ratio actually seen by the injected gas is much lower than the freestream value. For example, a Mach 4 air stream with static conditions of 300 K and 101 kPa will have a dynamic pressure of 1131 kPa. After passing through a normal shock, the static conditions will be 1214 K and 1869 kPa with a dynamic pressure of only 247 kPa, a 78% reduction in dynamic pressure. Application of the 1-D, inviscid compressible flow equations for a normal shock is not sufficient to correct the dynamic pressure ratio effect since the bow shock is only normal over a portion of the plume. An empirical method lends itself to more practical implementation.

It was shown in figure 5-1 that for injection into Mach 4 air the near-field penetration was much deeper than for injection at lower Mach numbers, but the far-field

penetration did not increase as rapidly. The increased near-field penetration is explained above and the decreased rate of far-field penetration is logically due to the greater free stream momentum, which at this point is only minimally altered by compressibility.

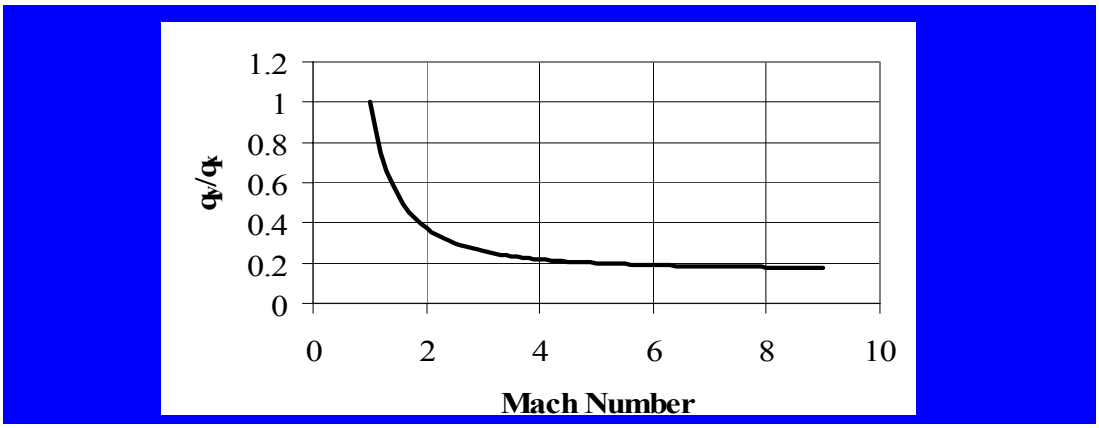

Figure 5-5. Dynamic Pressure Ratio Across a Normal Shock versus Mach number.

Despite increased penetration from the wall when the Mach number is low supersonic and the BL is thick, the penetration out of the BL and into the free stream is decreased by a thick BL. The strong, nearly normal bow shock is absent at low supersonic Mach number and thick BL. The supersonic freestream interacts with the deflected plume by forming a weaker oblique shock. With the weakened virtual obstruction of the injectant jet in the freestream, the vortex generation essential to effective bulk mixing processes is weakened. The resulting flow approaches the case of tangential, rather than transverse injection.

When the supersonic Mach number is high, much of the BL flow is also supersonic, so a strong bow shock extends deep into the BL with consequent low dynamic pressure downstream of the bow shock leading to increased penetration. The drop in dynamic pressure across the shock wave is more effective at increasing

penetration than velocity reduction in the BL. This explains the decreased effect of BL thickness on improving penetration as Mach number increases.

CHAPTER 6
CONCLUSIONS

This study has evaluated the penetration of gas jets into supersonic flows with thick boundary layers over various Mach numbers. Comparison with previous studies shows the following:

- Transverse jet penetration is dependent on q_j/q_a, x/D, δ/D and air Mach number. Among the parameters under the designer's control q_j/q_a has the strongest effect. The Mach number will modify the impact of the other variables and can have a dramatic effect on penetration which was not previously recognized.

- Generally, increased air Mach number results in increased penetration due to greater dynamic pressure reduction downstream of stronger shock waves.

- The effect of the boundary layer thickness on increasing near-field jet penetration is significant at low supersonic Mach numbers but decreases with increased Mach number.

- Deeper near-field penetration results in stronger vortex formation, which is known to enhance mixing and spreading.

- The effect of molecular weight ratio on penetration is small and not monotonic. The effect of Reynolds number is negligible.

LIST OF REFERENCES

1. Glass, C. E., "A Parametric Study of Jet Interactions with Rarefied Flow," *21st International Symposium on Rarefied Gas Dynamics,* edited by R. Brun, R. Campargue, R. Gatingnol, and J. C. Lengrand, Cepadues Editions, Toulouse France, 1998, Vol. 1, pp 615-622.

2. Kaufman, Louis G. II, "Hypersonic Flows Past Transverse Jets," *Journal of Propulsion and Power,* Vol. 4, No. 9, September 1967, pp 1230-1235.

3. Schetz, J., Billig, F., "Penetration of Gaseous Jets Injected into a Supersonic Stream," *Journal of Spacecraft and Rockets,* Vol. 3, No. 11, November 1966, pp 1658-1665.

4. Rogers, R. C., "A Study of the Mixing of Hydrogen Injected Normal to a Supersonic Airstream," NASA TN D-6114, 1971.

5. Owens, M., Tehranian, S., Segal, C. and Vinogradov, V., "Flame-Holding configurations for Kerosene Combustion in a Mach 1.8 Airflow," *Journal of Propulsion and Power,* Vol. 14, No. 4, July-August 1998, pp 456-461.

6. Gallimore, S., Jabobsen, L., O'Brien, W. and Schetz, J., "Operational Sensitivities of an Integrated Scramjet Ignition/Fuel Injection System," *Journal of Propulsion and Power,* Vol. 19, March-April 2003, pp183-189.

7. Parent, B. and Sislian, J., "Effect of Geometrical Parameters on the Mixing Performance of Cantilevered Ramp Injectors," *AIAA Journal,* Vol. 41, No. 3, pp 448-456.

8. F. H. Falempin, "Scramjet Development in France," *Scramjet Propulsion,* E. T. Curran and S. N. B. Murthy Editors, Progress in Astronautics and Aeronautics, AIAA, Washington D. C., 2000, vol. 189, pp 47-117.

9. McClinton, C. R., "Effect of Ratio of Wall Boundary-Layer Thickness to Jet Diameter on Mixing of a Normal Hydrogen Jet in a Supersonic Stream," NASA TM X-3030, June 1974, pp 1-42.

10. Gruber, M. R., Nejad, A. S., Chen, T. H. and Dutton, J. C., "Transverse Injection From Circular and Elliptic Nozzles into a Supersonic Crossflow," *Journal of Propulsion and Power,* Vol. 16, No. 3, May-June 2000, pp 449-457.

11. Ben-Yakar, A. and Hanson, R., "Experimental Investigation of Flame-Holding Capability of Hydrogen Transverse Jet in Supersonic Cross-flow," 27th Symposium (International) on Combustion/The Combustion Institute, 1998, pp 2173-2180.

12. Turns, S. R., *An Introduction to Combustion: Concepts and Applications,* Second Edition, McGraw-Hill, Boston, 2000, pp 84-88.

13. Dimotakis, P. E., "Turbulent Free Shear Layer Mixing and Combustion," *High Speed Flight Propulsion Systems,* in *Progress in Astronautics and Aeronautics*, AIAA, Washington D. C., 1991, Vol. 137, pp 265-340.

14. Billig, F. S., "Research on Supersonic Combustion," *Journal of Propulsion and Power,* Vol. 9, No. 4, July-August 1993, pp 499-520.

15. Seiner, J. , Dash, S. and Kenzakowski, D., "Historical Survey on enhanced Mixing in Scramjet Engines," *Journal of Propulsion and Power,* Vol. 17, No. 6, November-December 2001, pp 1273-1286.

16. Northam, G. B., Greenberg, I., Byington, C. S. and Caprotti, D. P., "Evaluation of Parallel Injector Configurations for Mach 2 Combustion," *Journal of Propulsion and Power,* Vol. 8, No. 2, March-april 1992, pp 491-499.

17. Owens, M. G., Segal, C. and Auslander, A. H., "Effects of Mixing Schemes on Kerosene Combustion in a Supersonic Airstream," *Journal of Propulsion and Power,* Vol. 13, No. 4, July-August 1997, pp 525-531.

18. McClinton, C. R., "The Effect of Injection angle on the Interaction Between Sonic Secondary Jets and a Supersonic Free Stream," NASA TN D-6669, February 1972.

19. Gaffney, R. L. Jr. and Korte, J., "Analysis and Design of Rectangular Cross-Section Nozzles For Scramjet Engine Testing," *AIAA Aerospace Science Meeting and Exhibit,* 5-8 January 2004, AIAA 2004-1137, pp 1-16.

20. Hersch, M., Povinelli, L. and Povinelli, F., "A Schlieren Technique for Measuring Jet Penetration into a Supersonic Stream," *Journal of Spacecraft and Rockets,* Vol. 7, No. 6, June 1970, pp 755-756.

21. Settles, G. S., *Schlieren and Shadowgraph Techniques, Visualizing Phenomena in Transparent Media,* Springer-Verlag, Berlin, 2001.

22. Swithenbank, J., Eames, I., Chin, S., Ewan, B., Yang, Z., Cao, J. and Zhao, X., "Turbulence Mixing in Supersonic Combustion Systems," AIAA Paper 89-0260, January 1989.

23. Torrence, M. G., "Effect of Injectant Molecular Weight on Mixing of a Normal Jet in a Mach 4 Airstream," NASA TN D-6061, January 1971, pp 1-104.

24. Povinelli, F. P. and Povinelli, L. A., "Correlation of Secondary Sonic and Supersonic Gaseous Jet Penetration into Supersonic Crossflows," NASA TN D-6370, June 1971, pp 1-20.

25. Billig, F. S., Orth, R. C. and Lasky, M., "A Unified Analysis of Gaseous Jet Penetration," *AIAA Journal,* Vol. 9, No. 6, June 1971, pp 1048-1058.

BIOGRAPHICAL SKETCH

Ron Portz was born in Rockledge, Florida, on May 31, 1965. He is a 1983 honor graduate of Cocoa High School, where he excelled in academic and artistic competition. He was both a National Merit Scholarship Finalist and a Scholastic Art Awards Gold Key recipient.

Mr. Portz served two years as a missionary for the Church of Jesus Christ of Latter Day Saints from 1986 to 1988 whereupon he resumed his academic career, graduating from the University of Florida in 1991 with a Bachelor of Science degree in Mechanical Engineering.

Mr. Portz has been happily married to the former Pamela Pierson since May 12, 1990. The couple currently have two adopted sons, Elijah and Samuel.

Following college graduation Mr. Portz worked for Rockwell International and The Boeing Corporation as a Test Engineer and a Depot Engineer for the Space Shuttle Main Propulsion System, Attitude Control System and Environmental Control/Life-Support System at NASA's Shuttle Logistics Depot in Cape Canaveral, Florida. In 1998, Mr. Portz began work for Orbital Sciences Corporation in Chandler, Arizona. His work responsibilities included the design, assembly, test and post-flight analysis of cold-gas, solid and liquid propellant propulsion systems. He is the recipient of multiple awards and recognitions for the quality of his work.

In 2003, Mr. Portz returned to the University of Florida to pursue a graduate degree in mechanical engineering. The University of Florida had been selected to lead the

Institute for Future Space Transport, which was described as paving the way for design of second and third generation reusable launch vehicles to replace the Space Shuttle. As space transportation has occupied the majority of his professional life and its future is precarious, he determined to participate in this program in the hope of applying his practical experience to provide needed direction to the industry. He is grateful for the opportunity to return to school and improve the depth of his academic knowledge.